

RESEARCH ARTICLE | MARCH 31 2025

Long spin-1/2 noble gas coherence times in mm-sized anodically bonded batch-fabricated ^3He - ^{129}Xe - ^{87}Rb cells

M. E. Limes   ; N. Dural; M. V. Romalis; E. L. Foley  ; T. W. Kornack; A. Nelson; L. R. Grisham

 Check for updates

Appl. Phys. Lett. 126, 134001 (2025)

<https://doi.org/10.1063/5.0245061>

 CHORUS



View Online



Export Citation

Articles You May Be Interested In

Transforming underground to surface mining operation – A geotechnical perspective from case study

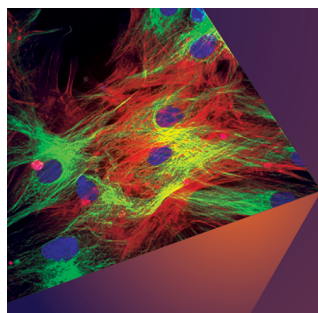
AIP Conference Proceedings (November 2021)

Monthly prediction of rainfall in nickel mine area with artificial neural network

AIP Conference Proceedings (November 2021)

Estimation of Karts groundwater based on geophysical methods in the Monggol Village, Saptosari District, Gunungkidul Regency

AIP Conference Proceedings (November 2021)



Applied Physics Letters

Special Topics Open for Submissions

[Learn More](#)

Long spin-1/2 noble gas coherence times in mm-sized anodically bonded batch-fabricated ^3He - ^{129}Xe - ^{87}Rb cells

Cite as: Appl. Phys. Lett. **126**, 134001 (2025); doi: 10.1063/5.0245061

Submitted: 23 October 2024 · Accepted: 3 February 2025 ·

Published Online: 31 March 2025



View Online



Export Citation



CrossMark

M. E. Limes,^{1,a)} N. Dural,¹ M. V. Romalis,¹ E. L. Foley,² T. W. Kornack,² A. Nelson,² and L. R. Grisham^{2,b)}

AFFILIATIONS

¹Department of Physics, Princeton University, Princeton, New Jersey 08544, USA

²Twinleaf LLC, Princeton, New Jersey 08544, USA

^{a)}Author to whom correspondence should be addressed: mlimes@vt.edu

^{b)}Deceased, May 4, 2020.

ABSTRACT

As the only stable spin-1/2 noble gas isotopes, ^3He and ^{129}Xe are promising systems for inertial rotation sensing and searches for exotic spin couplings. Spin-1/2 noble gases have intrinsic coherence times in the order of hours to days, which allows for incredibly low frequency error of free-precession measurements. However, relaxation in miniature cells is dominated by interactions with the cell wall, which limits the performance of a chip-scale sensor that uses noble gases. While ^{129}Xe wall relaxation times have previously been limited to 10s of seconds in mm-sized cells, we demonstrate the first anodically bonded batch-fabricated cells with dual ^3He - ^{129}Xe isotopes and ^{87}Rb in a 6 mm³ volume with ^3He and ^{129}Xe T_2 coherence times of, respectively, 4 h and 300 s. We use these microfabricated cells in a dual noble gas comagnetometer and discuss its limits.

Published under an exclusive license by AIP Publishing. <https://doi.org/10.1063/5.0245061>

The research and commercial development of miniature high-performance atomic sensors^{1–5} has naturally driven interest in chip-scale systems for hyperpolarization of noble gas nuclear spins.^{6,7} Compact noble gas NMR systems are used in a variety of studies, including searches of short-range spin-dependent forces,⁸ inertial rotation sensing,^{9–13} magnetometry,¹⁴ and microfluidic detection.^{15,16} These applications use vapor cells that contain the readily available ^{129}Xe or ^{131}Xe that are hyperpolarized by spin exchange with optically pumped alkali metals. Noble gas nuclei are notable for having extraordinarily long T_2 coherence times while having high densities, making the quantum projection frequency noise $\delta\omega = 1/\sqrt{T_2 N t}$ well below pHz levels,¹⁷ with N being the number of nuclei sampled and t being the measurement time. The potential of noble gases for rotation measurements has long been considered,^{18–20} but more than one simultaneous measurement is needed to discern rotations of the apparatus from changes in the local magnetic field. Thus, the use of a comagnetometer that samples the same magnetic field in the same volume is advantageous for rotation measurements done in a compact and cost-effective package. In principle, the spin-1/2 isotopes ^{129}Xe or ^3He ^{21–23} are the best candidates for systematic-free rotation measurements, as higher-spin isotopes like ^{131}Xe or ^{21}Ne are susceptible to additional

frequency shifts and relaxation mechanisms that can be deleterious.^{24–28} Detection of nuclear spins at a quantum shot noise level is difficult to achieve. A popular and sensitive detection method that takes advantage of the wavefunction overlap of the optically addressable electronic state of an alkali metal with a noble gas nuclei.^{29,30} While backaction and relaxation from the alkali on the noble gas must be mitigated,^{31,32} this method of detection is convenient because Rb alkali vapor is already present in these systems to hyperpolarize ^3He and ^{129}Xe through spin-exchange optical pumping.

Spin-1/2 noble gases intrinsically decohere very slowly through intraspecies collisional processes that form transient or persistent dimers, which allow for dipole–dipole and spin-rotation relaxation.^{33–35} Various extrinsic factors that cause nuclear relaxation include diffusion through magnetic field gradients, spin exchange, and spin destruction of the noble gases with warm alkali vapors, and relaxation due to the cell wall. Given a particular coating or cell surface, the characteristic wall relaxation time T_{wall} scales linearly with surface-to-volume ratio and follows an Arrhenius temperature dependence. In small cells with a large surface-to-volume ratio, the noble gas coherence times are often limited by interactions with the cell walls, with past studies showing ^{129}Xe relaxation of 10s of seconds.¹¹

We demonstrate batch fabrication of stemless anodically bonded cells that have a well-defined geometry and contain ^3He and ^{129}Xe with nuclear-spin coherence times of 4 hours and 300 s, respectively, a significant improvement in the ^{129}Xe coherence time for micro-fabricated cells and the first detection of ^3He signals in such cells. We then use these cells as a free-precession dual noble gas comagnetometer in a laboratory-sized prototype for a chip-scale gyroscope, achieving a stability of $0.2^\circ/\text{h}$ at 48 h.

For this study we make stemless cells shown in Fig. 1 by using a silicon wafer of thickness 2 mm, drilled with an array of 2 mm holes, machined with two 0.2 mm thick SD-2 aluminosilicate glass plates on each side.^{1,36} The wafer and glass are baked under high vacuum, which, along with cleanliness, is crucial to obtain long ^{129}Xe lifetimes. We first bond glass to one side of the wafer, and then introduce 99.9% isotopically enriched ^{87}Rb metal into the cells. Then the other side of the wafer is bonded to enclose the cell under a 187:0.87:10.7 kPa (approximately 1400:6.5:80 Torr) ^3He : ^{129}Xe : N_2 gas mixture in the bonding chamber. N_2 is included for quenching during optical

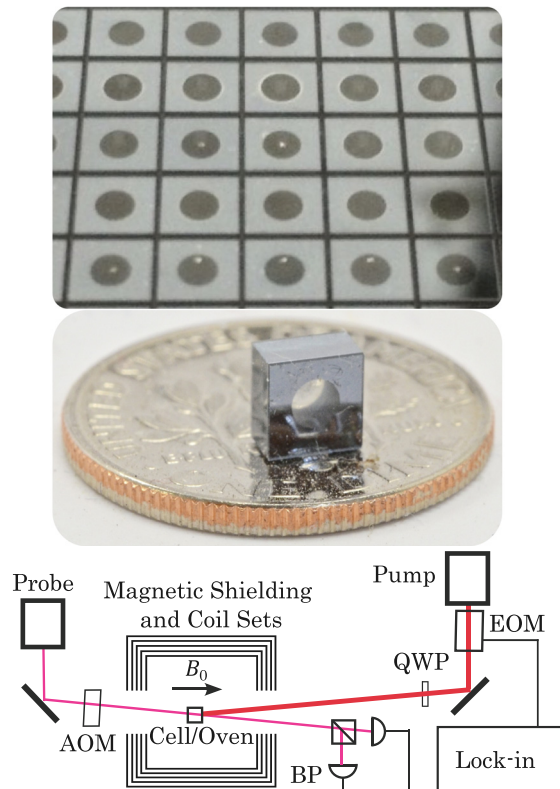


FIG. 1. Drilled silicon wafers can be filled with a variety of noble gases and enriched alkali isotopes, then anodically bonded and diced to make many uniform batch-fabricated vapor cells. We fill cells with ^3He - ^{129}Xe - ^{87}Rb - N_2 for use in a dual noble gas comagnetometer detected by an *in situ* alkali magnetometer and use long noble gas relaxation times to study a low-drift chip-scale gyroscope. In this study, twelve vapor cells across two wafers informed the presented results. For detection of the noble gases, we use co-linear probe and pump beams, with pump helicity flipped by an electro-optical modulator (EOM) and probe shuttered with an acousto-optical modulator (AOM), along with a fast ^{87}Rb π pulse train applied with small Helmholtz coils.

pumping of ^{87}Rb . Heat applied during bonding can cause buffer gas pressure loss in cells of up to 30%; we check the ^3He and ^{87}Rb densities by measuring the Rb absorption spectrum of the probe laser. A cryogenic storage system reclaims ^3He from the bonding chamber, enabling a pathway for fabricating many low-cost devices. Anodically bonded glass on machined silicon also allows for excellent control of the cell geometry. Typical glass-blown or optically contacted cells have a glass stem for cell filling and sealing,^{10,37} which creates an inherent asymmetry in the cell shape. Some are able to lessen cell stem effects by plugging the stem with alkali metal³⁸ or a small piece of movable glass.³⁹ Others have made stemless cells by allowing ^3He to diffuse through quartz walls at a high temperature.⁴⁰ The cell shape is an important consideration for precision measurements and chip-scale sensors that use noble gas precession frequency measurements, as it affects the long-range dipolar magnetic interactions between spin-polarized nuclei.⁴¹ Such interactions cause significant frequency shifts in precision comagnetometer measurements,⁴² where long-term drifts can be correlated with placement and magnitude of noble gas polarization.^{43–47} To study this dipolar effect, we recently used our cell fabrication process to make a slight wedge in the Si wafer to vary the height-to-diameter aspect ratios across many cells. We demonstrated the existence of an optimal aspect ratio that nulls the dipolar effect, as well as the existence of nuclear J -coupling between different noble gases ^3He - ^{129}Xe .⁴⁴ This J -coupling in principle also provides a mechanism for relaxation and polarization transfer between the different noble gas species, although this has not yet been directly observed.

We include ^{87}Rb in the cells in order to polarize nuclear spins by spin-exchange with ^{87}Rb that is polarized by optical pumping using a circularly polarized laser beam parallel to a longitudinal bias magnetic field $B_0 = 0.5 \mu\text{T}$, within a set of custom five-layer mu-metal magnetic shielding. We also detect noble gas spin precession with a ^{87}Rb magnetometer,^{31,48,49} which gives a high signal-to-noise ratio due to wavefunction overlap of the ^{87}Rb with the noble gases.^{50–53} Since the cells have only a single optical axis, counter-propagating pump and probe beams are used with fast ^{87}Rb magnetic field π pulses to make a pulse train magnetometer similar to that described in Refs. 31 and 44. For ^{87}Rb magnetometer operation, the polarization of a 795 nm pump laser is alternated between σ^+ and σ^- light at 13 kHz by an EOM. Synchronous $2 \mu\text{s}$ long magnetic field pulses along the y axis (or any axis in the transverse plane) quickly Rabi flop the ^{87}Rb polarization back and forth along B_0 . If the pulses are sufficiently fast and short, they can suppress alkali-alkali spin-exchange relaxation as well as precession of ^{87}Rb spins around B_0 .³¹ The ^{87}Rb polarization along B_0 is detected with a probe beam that is detuned off the $D1$ resonance, passing through the cell to a balanced polarimeter. The probe laser is shuttered by an AOM to open only during π pulses to mitigate probe broadening. A DC or low frequency B_y field parallel to the direction of the fast pulses delays or advances the ^{87}Rb signal zero-crossing during the π Rabi flop. This signal is measured by a lock-in amplifier referenced to half the EOM frequency with the lock-in output proportional to B_y . The sensitivity of the ^{87}Rb magnetometer is $300 \text{ fT}/\sqrt{\text{Hz}}$. We use sub-mW power from Photodigm DBR lasers through the active volume, similar to the powers from commercial VCSEL laser packages.

Although self-relaxation for the noble gases in our conditions yields coherence times of hundreds of hours for both ^{129}Xe and ^3He , our system is dominated by wall relaxation and Rb-noble gas interactions. To study ^{129}Xe relaxation mechanisms, we first spin-exchange

optically pump the ^{129}Xe along the bias field for 30–50 s, and have negligible ^3He polarization. A tipping pulse then places ^{129}Xe transverse to B_0 and its precession is detected with the pulse train ^{87}Rb magnetometer. A representative signal from the lock-in amplifier is shown in Fig. 2(a). We fit a given dataset to the function $A \exp(-t/T_2) \sin(\omega_{\text{Xe}}t)$ to extract T_2 , and show $^{129}\text{Xe} 1/T_2$ as a function of cell temperature and Rb density in Fig. 2(b). In this cell, we find the Rb absorption FWHM of 23.4 ± 1 GHz corresponding to roughly 1000 Torr ^3He .⁵⁴ From the slope in Fig. 2(b) we find a Rb–Xe spin-exchange rate of $(7.8 \pm 0.7) \times 10^{-16} \text{ cm}^3/\text{s}$. This value is in agreement with a calculation of the spin-exchange rate $7.2 \times 10^{-16} \text{ cm}^3/\text{s}$ based on previously measured cross sections.^{55,56} The relaxation rate does not change significantly from the Rb–Xe spin-exchange rate across our temperature range, so we neglect any Arrhenius temperature dependence in our analysis. The inset of Fig. 2(b) shows the Rb magnetometer can shorten $^{129}\text{Xe} T_2$ by causing a Rb polarization gradient that ^{129}Xe diffuses through. The additional relaxation depends on the ^{87}Rb pump laser power and the accuracy of $^{87}\text{Rb} \pi$ pulses. Increasing the $^{87}\text{Rb} \pi$ pulse repetition rate decreases this relaxation because the Rb gradient is reversed more rapidly. For accurate T_2 measurements, we use proper π pulses and low pump power. The ^3He coherence exceeds $^{129}\text{Xe} T_2$ by at least an order of magnitude, thus sufficient for our comagnetometer operation. Tests were completed over the course of roughly 6 months with no observed cell degradation.

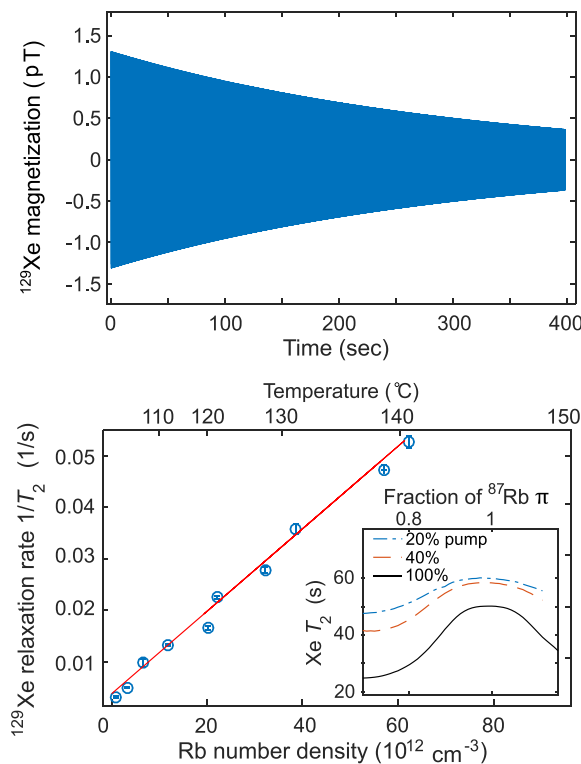


FIG. 2. Top: Spin precession signal from ^{129}Xe at $73.3 \pm 0.1^\circ\text{C}$ shows a relaxation time of $T_2 = 308 \pm 1$ s. Bottom: The dependence of $^{129}\text{Xe} T_2$ on the Rb number density. The inset shows that at 120°C ^{87}Rb pump light intensity and deviations of the alkali magnetometer π pulse amplitude from optimal conditions shorten $^{129}\text{Xe} T_2$ due to Xe diffusion in a ^{87}Rb polarization gradient.

To study the feasibility of these long noble gas lifetime cells in a compact gyroscope, we operate the noble gases in a free-precession comagnetometer, similar to measurements in Ref. 31 that were with larger glass-blown cells. For these measurements we hyperpolarize ^3He and ^{129}Xe along a bias field $B_0 = 0.5 \pm 0.1 \mu\text{T}$ that is co-linear to the pump and probe beams. We then apply a tipping pulse that places ^3He and ^{129}Xe spins in a plane transverse to B_0 . The ^{87}Rb pulse train magnetometer detects the precession of both noble gases about B_0 as shown in Fig. 3. To find the rotation rate for a given shot with both measurement styles, we first find the effective free-precession frequencies of the noble gases $\omega_{\text{He}} = \gamma_{\text{He}}B_0 + \Omega$ and $\omega_{\text{Xe}} = \gamma_{\text{Xe}}B_0 + \Omega$. We extract the rotation rate Ω by taking the ratio $f_r = \omega_{\text{He}}/\omega_{\text{Xe}}$ and finding $\Omega = \omega_{\text{Xe}}(\gamma_r - f_r)/(\gamma_r - 1)$ with $\gamma_r = \gamma_{\text{He}}/\gamma_{\text{Xe}} = 2.754\,081\,3(3)$.⁵⁷ After a measurement, the noble gas spins are placed back along the bias field by dumping feedback from the lock-in signal.⁵⁸ Repeating this sequence, we run the comagnetometer for an extended period of time to determine its sensitivity and long-term stability. In Fig. 4, we compare the Allan deviations for a Ramsey-style sequence with active Rb depolarization and for measurements with the Rb π pulse train magnetometer continuously running. For the Ramsey-style measurement, each shot takes about 115 s, with a 25 s initial and 45 s final detection period (giving a bandwidth of 4.3 mHz). We fit the detection period signals to decaying sine waves to determine the phases ϕ_1 and ϕ_2 with which the spins enter and leave the dark detection period $T_d = 45$ s. Assuming there are no significant changes in the precession frequency,

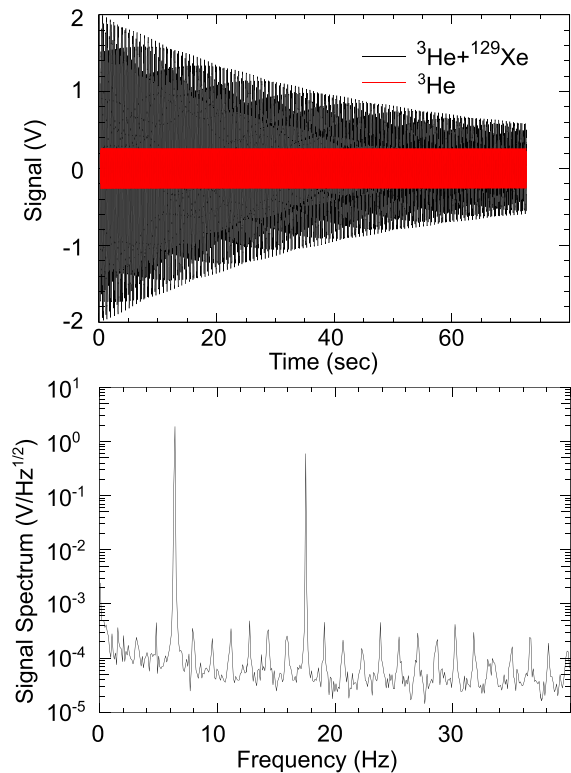


FIG. 3. Top: Time-domain ^3He - ^{129}Xe free-precession comagnetometer signals detected with an *in situ* ^{87}Rb magnetometer at an operating temperature of 120°C . Bottom: Spectral density of comagnetometer in mm-scale cells.

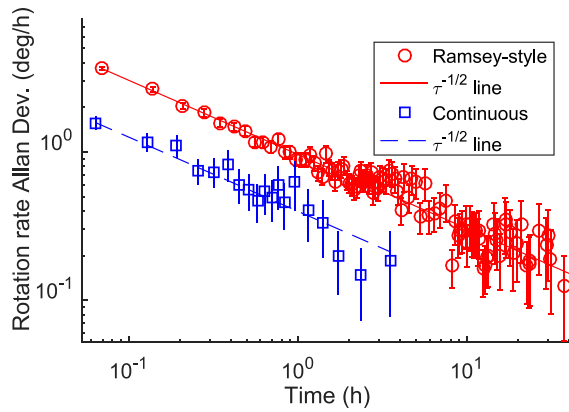


FIG. 4. Our system stability is shown with Allan deviations (see IEEE Standard 952-1997) for ^3He - ^{129}Xe comagnetometer detected with an *in situ* ^{87}Rb magnetometer. We compare the precision of a continuous-mode pulsed magnetometer operation with a Ramsey-style sequence that has an Rb-noble gas decoupling and dark period separating two detection periods. Both datasets are taken in a batch-fabricated anodically bonded cell at 120°C , and have a practical limit of achievable steady-state ^3He polarization. Note: $1\text{ rad/s} \approx 206\,393^\circ/\text{h}$, and $\tau^{-1/2}$ lines are guides to the eye to indicate an angular random walk.

we find the in-the-dark free-precession frequencies of the noble gases by taking $\omega = \Delta\phi/\Delta t = (2n\pi + \phi_2 - \phi_1)/T_d$, where n is an integer determined from an estimate of the precession frequency. During the dark period, a two-axis decoupling pulse train is used to mitigate noble gas frequency shifts due to ^{87}Rb back polarization and nulls Bloch-Siegert shifts introduced by the pulse train.³¹ For continuous measurements, each shot lasts about 50 s, and we fit two decaying sine waves to find ω_{Xe} and ω_{He} . In both measurement styles, we find frequency uncertainty is limited by the ^3He frequency error due to low steady-state ^3He magnetization at a temperature that allows for long ^{129}Xe T_2 , as higher temperatures cause greater Rb-Xe relaxation. The Ramsey-style measurement integrates for more than a day, longer than the continuous method by about an order of magnitude, with both methods reaching around $0.2^\circ/\text{h}$ precision before drifting. The uncertainties achieved here are about an order of magnitude worse than that achieved in the same system for glass-blown cells with 100 times larger volume used in Ref. 31. Using microfabricated cells with higher ^3He pressure would improve the performance, as in the current cells the small steady-state magnetization becomes insufficient with practical shot-to-shot pumping periods. To determine expected gyroscope performance, we can use Cramér-Rao lower bounds (CRLB) of a decaying sine wave⁵⁹⁻⁶¹ to estimate a lower bound for the rotation error

$$\delta\Omega = \frac{1}{\gamma_r - 1} \sqrt{\gamma_r^2 \delta\omega_{\text{Xe}}^2 + \delta\omega_{\text{He}}^2}. \quad (1)$$

For a decaying sine wave,

$$\begin{aligned} \frac{\delta\omega}{2\pi} &= \frac{\sqrt{12C}}{2\pi T_m^{3/2} A/\rho} [\text{Hz}], \\ \delta\phi &= \frac{2\sqrt{D}}{T_m^{1/2} A/\rho} [\text{rad}], \end{aligned} \quad (2)$$

where T_m is the measurement time and A is the initial sine wave amplitude in volts (V) and ρ is the spectral density of white Gaussian

noise ($\text{V}/\text{Hz}^{1/2}$). C and D are factors depending on the measurement and relaxation time T_m and T_2 that both approach unity as $T_2 \rightarrow \infty$. For Ramsey-style detection in the limit of long T_2 , the optimal detection intervals are $1/6$ of the total measurement time and the overall statistical sensitivity is three times worse than for continuous detection of equal time. For finite relaxation one can show that

$$\begin{aligned} C &= \frac{T_m^3 (e^{\frac{2T_m}{T_2}} - 1)}{3T_2^3 \cosh\left(\frac{2T_m}{T_2}\right) - 3(T_2^3 + 2T_2 T_m^2)}, \\ D_1 &= \frac{e^{\frac{2T_m}{T_2}} T_m (-2T_2 T_m + 2T_m^2 + T_2^2) - T_2^2 T_m}{2T_2^3 \cosh\left(\frac{2T_m}{T_2}\right) - 2(2T_2 T_m^2 + T_2^3)}, \\ D_2 &= \frac{T_2^2 T_m (e^{\frac{2T_m}{T_2}} - 1) - 2T_m^2 - 2T_2 T_m^2}{2T_2^3 \cosh\left(\frac{2T_m}{T_2}\right) - 2(2T_2 T_m^2 + T_2^3)}, \end{aligned} \quad (3)$$

where D_1 is used for estimating the trailing phase of the first detection period and D_2 for the leading phase of the second period. Using the signal height, noise, and relaxation times from Fig. 3, and considering detection, in-the-dark, and shot-to-shot times used in Fig. 4, we find a Cramér-Rao frequency uncertainty lower bound that corresponds to an angular random walk at one hour of $0.094^\circ/\sqrt{\text{h}}$ for a Ramsey-style measurement and $0.056^\circ/\sqrt{\text{h}}$ for continuous operation, both about an order of magnitude better than we realized experimentally.

In conclusion, we demonstrate the fabrication of miniature stemless anodically bonded vapor cells containing ^3He , ^{129}Xe , ^{87}Rb , and N_2 with long ^{129}Xe and ^3He coherence times. We use these cells in a dual noble gas comagnetometer detected by an *in situ* ^{87}Rb pulse train magnetometer, and study the long-term stability of the system. Though far from fundamental limits, this system has great potential for high-precision, accurate³¹ rotation measurements in a small, low-cost package.

This work was funded by DARPA (Defense Advanced Research Project Agency) under Contract No. FA8650-13-1-7326 and NSF Grant No. 1404325.

AUTHOR DECLARATIONS

Conflict of Interest

The authors have no conflicts to disclose.

Author Contributions

M. E. Limes: Conceptualization (equal); Data curation (equal); Formal analysis (equal); Investigation (equal); Methodology (equal); Software (equal); Validation (equal); Visualization (equal); Writing – original draft (equal); Writing – review & editing (equal). **N. Dural:** Conceptualization (supporting); Investigation (supporting). **M. V. Romalis:** Conceptualization (lead); Data curation (supporting); Formal analysis (equal); Funding acquisition (lead); Investigation (supporting); Methodology (equal); Project administration (lead); Resources (lead); Supervision (lead); Validation (lead); Writing – original draft (supporting); Writing – review & editing (supporting). **E. L. Foley:** Methodology (supporting); Resources (supporting). **T. W. Kornack:** Methodology (supporting); Resources (supporting).

A. Nelson: Methodology (supporting); Resources (supporting). **L. R. Grisham:** Methodology (equal); Resources (equal).

DATA AVAILABILITY

The data that support the findings of this study are available from the corresponding author upon reasonable request.

REFERENCES

- ¹L.-A. Liew, S. Knappe, J. Moreland, H. Robinson, L. Hollberg, and J. Kitching, "Microfabricated alkali atom vapor cells," *Appl. Phys. Lett.* **84**, 2694 (2004).
- ²S. Knappe, P. D. D. Schwindt, V. Gerginov *et al.*, *J. Opt. A: Pure Appl. Opt.* **8**, S318 (2006).
- ³J. Kitching, "Chip-scale atomic devices," *Appl. Phys. Rev.* **5**, 031302 (2018).
- ⁴M. Limes, E. Foley, T. Kornack, S. Caliga, S. McBride, A. Braun, W. Lee, V. Lucivero, and M. Romalis, "Portable magnetometry for detection of biomagnetism in ambient environments," *Phys. Rev. Appl.* **14**, 011002 (2020).
- ⁵J. P. McGilligan, K. R. Moore, A. Dellis, G. D. Martinez, E. de Clercq, P. F. Griffin, A. S. Arnold, E. Riis, R. Boudot, and J. Kitching, "Laser cooling in a chip-scale platform," *Appl. Phys. Lett.* **117**, 054001 (2020).
- ⁶M. Ledbetter, I. Savukov, D. Budker, V. Shah, S. Knappe, J. Kitching, D. Michalak, S. Xu, and A. Pines, "Zero-field remote detection of nmr with a microfabricated atomic magnetometer," *Proc. Natl. Acad. Sci. U. S. A.* **105**, 2286 (2008).
- ⁷R. Jiménez-Martínez, D. J. Kennedy, M. Rosenbluh, E. A. Donley, S. Knappe, S. J. Seltzer, H. L. Ring, V. S. Bajaj, and J. Kitching, "Optical hyperpolarization and nmr detection of ^{129}Xe on a microfluidic chip," *Nat. Commun.* **5**, 3908 (2014).
- ⁸M. Bulatowicz, R. Griffith, M. Larsen, J. Mirijanian, C. B. Fu, E. Smith, W. M. Snow, H. Yan, and T. G. Walker, "Laboratory search for a long-range t-odd, p-odd interaction from axionlike particles using dual-species nuclear magnetic resonance with polarized ^{129}Xe and ^{131}Xe gas," *Phys. Rev. Lett.* **111**, 102001 (2013).
- ⁹E. A. Donley, "Nuclear magnetic resonance gyroscopes," in *IEEE Sensors Proceedings* (IEEE, 2010) p. 17.
- ¹⁰M. Larsen and M. Bulatowicz, "Nuclear magnetic resonance gyroscope," in *IEEE International Frequency Control Symposium Proceedings* (IEEE, 2012).
- ¹¹T. Walker and M. Larsen, "Chapter eight—Spin-exchange-pumped {NMR} gyros," *Adv. At., Mol. Opt. Phys.* **65**, 373 (2016).
- ¹²G. Buchs, S. Karlen, T. Overstolz, N. Torcheboeuf, E. Onillon, J. Haesler, and D. L. Boiko, *AIP Conf. Proc.* **1936**, 020011 (2018).
- ¹³D. A. Thrasher, S. S. Sorensen, J. Weber, M. Bulatowicz, A. Korver, M. Larsen, and T. G. Walker, "Continuous comagnetometry using transversely polarized xe isotopes," *Phys. Rev. A* **100**, 061403 (2019).
- ¹⁴M. Bulatowicz and M. Larsen, "Compact atomic magnetometer for global navigation," in *IEEE/ION PLANS Proceedings* (IEEE, 2012), p. 1088.
- ¹⁵R. M. Noor, M. H. Asadian, and A. M. Shkel, "Design considerations for micro-glassblown atomic vapor cells," *J. Microelectromech. Syst.* **29**(1), 25–35 (2022).
- ¹⁶D. Kennedy, S. J. Seltzer, R. Jiménez-Martínez *et al.*, *Sci. Rep.* **7**, 43994 (2017).
- ¹⁷T. R. Gentile, P. J. Nacher, B. Saam, and T. G. Walker, "Optically polarized ^3He ," *Rev. Mod. Phys.* **89**, 045004 (2017).
- ¹⁸A. Kastler, "The hanle effect and its use for the measurements of very small magnetic fields," *Nucl. Instrum. Methods* **110**, 259 (1973).
- ¹⁹L. K. Lam, E. Phillips, E. Kanegsberg, and G. W. Kamin, "Application of CW single-mode GaAlAs lasers to Rb-Xe NMR gyroscopes," *Proc. SPIE* **412**, 272–276 (1983).
- ²⁰M. Mehring, A. Appelt, B. Menke, and P. Scheufler, *High Precision Navigation 91: Proceedings of the 2nd International Workshop on High Precision Navigation, Stuttgart and Freudenstadt, 1991*, edited by K. Linkwitz and U. Hangleiter (Dummler Verlag, 1992).
- ²¹T. E. Chupp, M. E. Wagshul, K. P. Coulter, A. B. McDonald, and W. Happer, "Polarized, high-density, gaseous ^3He targets," *Phys. Rev. C* **36**, 2244 (1987).
- ²²R. E. Stoner, M. A. Rosenberry, J. T. Wright, T. E. Chupp, E. R. Oteiza, and R. L. Walsworth, "Demonstration of a two species noble gas maser," *Phys. Rev. Lett.* **77**, 3971 (1996).
- ²³D. Bear, R. E. Stoner, R. L. Walsworth, V. A. Kostelecký, and C. D. Lane, "Limit on lorentz and CPT violation of the neutron using a two-species noble-gas maser," *Phys. Rev. Lett.* **85**, 5038 (2000).
- ²⁴T. E. Chupp and K. P. Coulter, "Polarization of ^{21}Ne by spin exchange with optically pumped rb vapor," *Phys. Rev. Lett.* **55**, 1074 (1985).
- ²⁵Z. Wu, W. Happer, and J. M. Daniels, "Coherent nuclear-spin interactions of adsorbed ^{131}Xe gas with surfaces," *Phys. Rev. Lett.* **59**, 1480 (1987).
- ²⁶T. E. Chupp, E. R. Oteiza, J. M. Richardson, and T. R. White, "Precision frequency measurements with polarized ^3He , ^{21}Ne , and ^{129}Xe atoms," *Phys. Rev. A* **38**, 3998 (1988).
- ²⁷R. Butscher, G. Wäckerle, and M. Mehring, "Nuclear quadrupole interaction of highly polarized gas phase ^{131}Xe with a glass surface," *J. Chem. Phys.* **100**, 6923 (1994).
- ²⁸E. A. Donley, J. L. Long, T. C. Liebisch, E. R. Hodby, T. A. Fisher, and J. Kitching, *Phys. Rev. A* **79**, 013420 (2009).
- ²⁹T. G. Walker and W. Happer, "Spin-exchange optical pumping of noble-gas nuclei," *Rev. Mod. Phys.* **69**, 629 (1997).
- ³⁰S. Appelt, A. B.-A. Baranga, C. J. Erickson, M. V. Romalis, A. R. Young, and W. Happer, "Theory of spin-exchange optical pumping of ^3He and ^{129}Xe ," *Phys. Rev. A* **58**, 1412 (1998).
- ³¹M. E. Limes, D. Sheng, and M. V. Romalis, *Phys. Rev. Lett.* **120**, 033401 (2018).
- ³²A. Korver, D. Thrasher, M. Bulatowicz, and T. G. Walker, "Synchronous spin-exchange optical pumping," *Phys. Rev. Lett.* **115**, 253001 (2015).
- ³³N. R. Newbury, A. S. Barton, G. D. Cates, W. Happer, and H. Middleton, "Gaseous ^3He magnetic dipolar spin relaxation," *Phys. Rev. A* **48**, 4411 (1993).
- ³⁴B. Chann, I. A. Nelson, L. W. Anderson, B. Driehuys, and T. G. Walker, " ^{129}Xe – Xe molecular spin relaxation," *Phys. Rev. Lett.* **88**, 113201 (2002).
- ³⁵B. C. Anger, G. Schrank, A. Schoeck, K. A. Butler, M. S. Solum, R. J. Pugmire, and B. Saam, "Gas-phase spin relaxation of ^{129}Xe ," *Phys. Rev. A* **78**, 043406 (2008).
- ³⁶A. Dellis, V. Shah, E. Donley, S. Knappe, and J. Kitching, *Opt. Lett.* **41**, 2775 (2016).
- ³⁷E. J. Eklund, A. M. Shkel, S. Knappe, E. Donley, and J. Kitching, "Glass-blown spherical microcells for chip-scale atomic devices," *Sens. Actuators, A* **143**, 175 (2008).
- ³⁸J. Lee, A. Almasi, and M. Romalis, "Improved limits on spin-mass interactions," *Phys. Rev. Lett.* **120**, 161801 (2018).
- ³⁹M. V. Balabas, T. Karaulanov, M. P. Ledbetter, and D. Budker, "Polarized alkali-metal vapor with minute-long transverse spin-relaxation time," *Phys. Rev. Lett.* **105**, 070801 (2010).
- ⁴⁰A. Maul, P. Blümler, W. Heil, A. Nikiel, E. Otten, A. Petrich, and T. Schmidt, *Rev. Sci. Instrum.* **87**, 015103 (2016).
- ⁴¹E. Stoltz, J. Tannenhauser, and P. Nacher, *J. Low Temp. Phys.* **101**, 839 (1995).
- ⁴²F. Allmendinger, W. Heil, S. Karpuk, W. Kilian, A. Scharth, U. Schmidt, A. Schnabel, Y. Sobolev, and K. Tullney, "New limit on lorentz-invariance- and cpt-violating neutron spin interactions using a free-spin-precession ^3He - ^{129}Xe comagnetometer," *Phys. Rev. Lett.* **112**, 110801 (2014).
- ⁴³M. V. Romalis, D. Sheng, B. Saam, and T. G. Walker, "Comment on "new limit on lorentz-invariance- and cpt-violating neutron spin interactions using a free-spin-precession ^3He - ^{129}Xe comagnetometer," *Phys. Rev. Lett.* **113**, 188901 (2014).
- ⁴⁴M. E. Limes, N. Dural, M. V. Romalis, E. L. Foley, T. W. Kornack, A. Nelson, L. R. Grisham, and J. Vaara, "Dipolar and scalar ^3He - ^{129}Xe frequency shifts in stemless cells," *Phys. Rev. A* **100**, 010501 (2019).
- ⁴⁵J. Vaara and M. V. Romalis, "Calculation of scalar nuclear spin-spin coupling in a noble-gas mixture," *Phys. Rev. A* **99**, 060501 (2019).
- ⁴⁶W. A. Terrano, J. Meinel, N. Sachdeva, T. E. Chupp, S. Degenkolb, P. Fierlinger, F. Kuchler, and J. T. Singh, "Frequency shifts in noble-gas comagnetometers," *Phys. Rev. A* **100**, 012502 (2019).
- ⁴⁷N. Sachdeva, I. Fan, E. Babcock, M. Burghoff, T. E. Chupp, S. Degenkolb, P. Fierlinger, S. Haude, E. Kraegeloh, W. Kilian, S. Knappe-Grüneberg, F. Kuchler, T. Liu, M. Marino, J. Meinel, K. Rolfs, Z. Salhi, A. Schnabel, J. T. Singh, S. Stuiber, W. A. Terrano, L. Trahms, and J. Voigt, "New limit on the permanent electric dipole moment of ^{129}Xe using ^3He comagnetometry and squid detection," *Phys. Rev. Lett.* **123**, 143003 (2019).
- ⁴⁸D. Sheng, A. Kabcenell, and M. V. Romalis, "New classes of systematic effects in gas spin comagnetometers," *Phys. Rev. Lett.* **113**, 163002 (2014).

- ⁴⁹E. Zhivun, M. Bulatowicz, A. Hryciuk, and T. Walker, "Dual-axis π -pulse magnetometer with suppressed spin-exchange relaxation," *Phys. Rev. Appl.* **11**, 034040 (2019).
- ⁵⁰S. R. Schaefer, G. D. Cates, T.-R. Chien, D. Gonatas, W. Happer, and T. G. Walker, "Frequency shifts of the magnetic-resonance spectrum of mixtures of nuclear spin-polarized noble gases and vapors of spin-polarized alkali-metal atoms," *Phys. Rev. A* **39**, 5613 (1989).
- ⁵¹M. V. Romalis and G. D. Cates, "Accurate ^3He polarimetry using the rb zeeman frequency shift due to the Rb- ^3He spin-exchange collisions," *Phys. Rev. A* **58**, 3004 (1998).
- ⁵²Z. L. Ma, E. G. Sorte, and B. Saam, "Collisional ^3He and ^{129}Xe frequency shifts in rb-noble-gas mixtures," *Phys. Rev. Lett.* **106**, 193005 (2011).
- ⁵³A. I. Nahlawi, Z. L. Ma, M. S. Conradi, and B. Saam, "High-precision determination of the frequency-shift enhancement factor in rb- ^{129}Xe ," *Phys. Rev. A* **100**, 053415 (2019).
- ⁵⁴M. V. Romalis, E. Miron, and G. D. Cates, "Pressure broadening of Rb D_1 and D_2 lines by ^3He , ^4He , N_2 , and Xe: Line cores and near wings," *Phys. Rev. A* **56**, 4569 (1997).
- ⁵⁵I. A. Nelson, "Physics of practical spin-exchange optical pumping," Ph.D. thesis (University of Wisconsin-Madison, 2001).
- ⁵⁶G. Schrank, Z. Ma, A. Schoeck, and B. Saam, "Characterization of a low-pressure high-capacity ^{129}Xe flow-through polarizer," *Phys. Rev. A* **80**, 063424 (2009).
- ⁵⁷W. Makulski, " ^{129}Xe and ^{131}Xe nuclear magnetic dipole moments from gas phase nmr spectra," *Magn. Reson. Chem.* **53**, 273 (2015).
- ⁵⁸O. Alem, K. L. Sauer, and M. V. Romalis, "Spin damping in an rf atomic magnetometer," *Phys. Rev. A* **87**, 013413 (2013).
- ⁵⁹T. E. Chupp, R. J. Hoare, R. L. Walsworth, and B. Wu, "Spin-exchange-pumped ^3He and ^{129}Xe Zeeman masers," *Phys. Rev. Lett.* **72**, 2363 (1994).
- ⁶⁰Y.-X. Yao and S. M. Pandit, "Cramer-rao lower bounds for a damped sinusoidal process," *IEEE Trans. Signal Process.* **43**, 878 (1995).
- ⁶¹C. Gemmel, W. Heil, S. Karpuk, K. Lenz, C. Ludwig, Y. Sobolev, K. Tullney, M. Burghoff, W. Kilian, S. Knappe-Grüneberg, W. Müller, A. Schnabel, F. Seifert, L. Trahms, and S. Baessler, "Ultra-sensitive magnetometry based on free precession of nuclear spins," *Eur. Phys. J. D* **57**, 303 (2010).